CRYSTAL GROWTH & DESIGN

Article

Cite This: *Cryst. Growth Des.* 2018, 18, 5210−5213

pubs.acs.org/crystal

Spatially Resolved X-ray Photoemission Electron Microscopy of Weyl Semimetal NbAs

Hongwen Liu,*[,†] Guanhua Zhang,[§] Pierre Richard,[†,∥,⊥,‡] Lingxiao Zhao,[†] Gen-Fu Chen,[†,∥,⊥] and Hong Ding*[,†,∥,⊥]

[†]Institute of Physics, Chinese Academy of Sciences, Beijing 100190, China

[§]Dalian Institute of Chemical Physics, Chinese Academy of Sciences, Dalian 116023, Liaoning China

[∥]School of Physics, University of Chinese Academy of Sciences, Beijing 100190, China

[⊥]Collaborative Innovation Center of Quantum Matter, Beijing, 100190, China

[‡]Institut Quantique, Université de Sherbrooke, 2500 boulevard de l'Université, Sherbrooke, Québec J1K 2R1, Canada

ABSTRACT: We utilized X-ray photoemission electron microscopy (XPEEM) and X-ray photoelectron spectroscopy (XPS) to investigate the crystal surface of Weyl semimetal NbAs. XPEEM images present white and black contrast in both the Nb 3d and As 3d core level spectra. Surface-sensitive XPS spectra indicate that the entire surface of the sample contains both surface states of Nb 3d and As 3d, in the form of oxides, and bulk states of NbAs. Estimated atomic percentage values n_{Nb}/n_{As} suggest that the surface is Nb-rich and different for white and black areas.

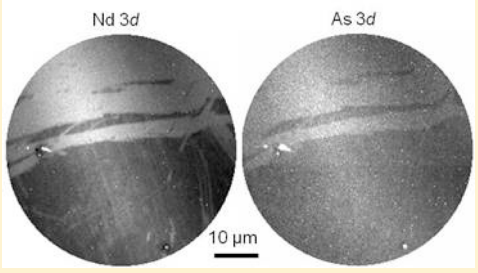

INTRODUCTION

In 1929, H. Weyl proposed that the massless solution of the Dirac equation represents a pair of new particles, the so-called Weyl fermions.[1] Their existence in particle physics remains elusive even after more than eight decades. However, theorists recently predicted that the Weyl fermions exist in the TaAs family of crystalline compounds (TaAs, NbAs, NbP, and TaP),[2] which was followed by their experimental observation by angle-resolved photoemission spectroscopy (ARPES).[3−7] Due to inversion symmetry-breaking, the surface electronic structure of these materials is characterized by an arclike topology connecting the surface projection of 24 Weyl nodes in the bulk band structure.[2] The discovery of the Weyl semimetals has received worldwide interest and it is believed to open a new area in condensed matter physics after graphene and the three-dimensional topological insulators.

The surface structure of the TaAs family of compounds is not fully understood. In principle, both (Ta,Nb) and (As,P) surface terminations are as likely to occur. This is consistent with Souma et al. claiming that the cleaved surface of NbP is a single domain with either a Nb or P surface termination.[8] In TaP, both types of surface terminations are also detected, but they coexist, indicating that the cleaved surface is not a single domain.[9] In contrast, Lv et al. report that for a cleaved surface of TaAs, only the As-termination is observed by ARPES.[3]

Motivated by the lack of understanding of the surface structure of the TaAs family of compounds, which is important to their topological properties, here we report a study of spatial-resolved X-ray photoemission electron microscopy (XPEEM) and X-ray photoelectron spectroscopy (XPS) of Weyl semimetal NbAs.

EXPERIMENTAL SECTION

The NbAs plate-like samples we studied were grown by chemical vapor transport. The crystal orientation has been determined by X-ray diffraction. Only the (0 0 4) and (0 0 8) peaks are detected, suggesting that the samples are single crystalline, which was also confirmed by Raman scattering measurements on samples from the same batch.[10] The NbAs crystal has a non-centrosymmetric structure corresponding to space group $I4_1md$ (109) and point group C_{4v}, as shown in Figure 1a. We utilize a commercial spectroscopic photoemission and low-energy electron microscope (SPELEEM from Elmitec Co. Ltd.) at the XPEEM endstation of the Dreamline (beamline 09U) at Shanghai Synchrotron Radiation Facility to record mirror electron microscopy (MEM), XPEEM images, and spatially resolved XPS. The energy resolution of the PEEM is 0.15 eV. The angle between the X-ray beam and the sample surface is 16°. Samples with a typical size of 0.4 × 0.4 × 0.08 mm^3 were cleaned in an

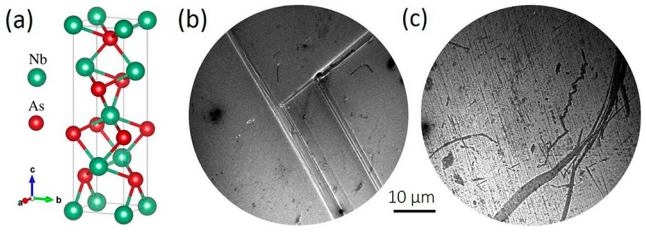

Figure 1. (a) Molecular structure of NbAs. (b) MEM at start voltage (V_{st}) = −0.25 V. (c) MEM at V_{st} = −0.56 V.

Received: April 28, 2018
Revised: July 1, 2018
Published: July 19, 2018

DOI: 10.1021/acs.cgd.8b00653
Cryst. Growth Des. 2018, 18, 5210−5213

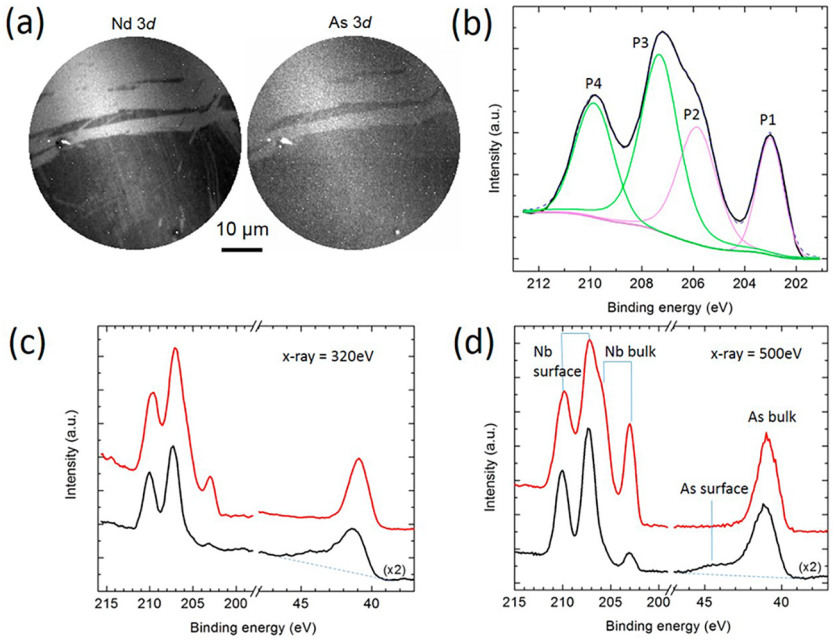

Figure 2. (a) Typical average XPEEM maps of NbAs sample. The photon energy is 320 eV. (b) Typical XPS spectrum of Nb 3d core level. Two sets of peaks, P1/P2 and P3/P4, are resolved. (c) Typical 3d core level spectra of Nb and As recorded with 320 eV photons. (d) Same as (c) but using 500 eV photons. The red curves in (c) and (d) have been extracted from the white area, whereas the black curves come from the black area.

ultrasonic bath, transferred in air into the SPELEEM chamber, and then annealed at 300 °C for 8 to 10 h to remove the adsorbates. We notice that all attempts to measure cleaved samples failed due to sample arcing. The typical base pressure in the main chamber was 3×10^{-10} Torr.

RESULTS AND DISCUSSION

MEM images reveal the surface potential as determined by topography, work function, and surface charge variations.[11] Taking advantage of higher lateral resolution, Figure 1b shows typical natural growth tracks with rectangular shape bundle steps on the NbAs surface, which are consistent with the (001) facet of NbAs. Dense and parallel segments and sharp contrast of patterns can be seen in Figure 1c, indicating that the surface is spatially resolved. We note that the surface does not produce a low-energy electron diffraction pattern, suggesting that it is amorphous.

The PEEM technique detects electrons emitted from atoms with kinetic energy $E_{kin} = h\nu - E_{bin} - \varphi$, where $h\nu$ is the photon energy and φ the work function.[12] Typically, $h\nu$ is fixed and E_{kin} is varied, which allows probing the chemical states of the emitting atoms by measuring the binding energies of their core electrons. The intensity of the photoemission signal is proportional to the number of emitters in the topmost layers within their energy-dependent escape depth, and thus provides straightforward and quantitative information about the chemical composition at the surface.

Figure 2a compares average XPEEM maps for kinetic energies tuned around the Nb 3d and As 3d core levels. The dark/bright contrast is inversed in MEM images (not shown here). The emitted flux and brightness contrast change with energy in the XPEEM maps. The maps recorded with energies close to the core levels have sharper brightness contrast. In our measurements, the image contrast for Nb is always sharper than for As, which may be caused by different photoemission cross sections or sensitivity factors. White and black areas coexist on the surface and the patterns do not follow the underlying topographies.

A typical XPS spectrum near the Nb 3d binding energy is shown in Figure 2b. The binding energy of Nb $3d_{5/2}$ electrons in NbAs is found between 202 and 204 eV, as compared to 202.0 eV in metallic Nb and 203.8 eV in NbN. Four peaks can be resolved, as illustrated by a Voigt fit. This corresponds to twice the number of peaks expected for bulk NbAs, indicating the existence of a second Nb site. Similarly, previous ARPES studies reported two As sites, as deduced by the observation of 4 core level peaks.[3,5,6] Here, we detect the As 3d core levels at 40.9 eV (Figure 2c,d). Due to a lower energy resolution than in the ARPES measurements, we can resolve clearly neither the $3d_{3/2}$ and $3d_{5/2}$ components, nor additional splitting. However, the peak shape is irregular, indicating that more than one peak is present.

In order to understand the nature of the two Nb sites, we use the PEEM capability of resolving the evolution of the Nb 3d core levels with respect to space. The P3 and P4 peaks at higher binding energy are observed systematically at every point and for all photon energies used. The intensity of the accompanying P1 and P2 (a shoulder) peaks at lower energy, however, strongly depends on the X-ray energy and local areas, and it sometimes nearly vanishes. More specifically, the P1 and P2 peaks have much weaker intensity in the dark areas in the XPEEM images in Figure 2a. This is well illustrated by the spectra displayed in Figure 2c,d. We thus assign the four peaks to two pairs: 203 eV (P1)/205.8 eV (P2), and 207.2 eV (P3)/209.9 eV (P4). Each pair has an energy splitting of ~2.7 eV, which is consistent to our expectation for the spin−orbit-split $3d_{5/2}$ and $3d_{3/2}$ levels of Nb 3d core levels.

Our results suggest that the P1 and P2 peaks are related to bulk NbAs states, while the P3 and P4 peaks, less bulk-sensitive, are associated with photoemission of Nb at the surface. To support this assumption, we performed XPS measurements from the same selected areas after adjusting the incident X-rays to 660, 580, and 480 eV. In the soft X-ray

DOI: 10.1021/acs.cgd.8b00653
Cryst. Growth Des. 2018, 18, 5210−5213

regime, the bulk sensitivity of the photoemission spectroscopies increases with photon energy. As shown in Figure 3, the

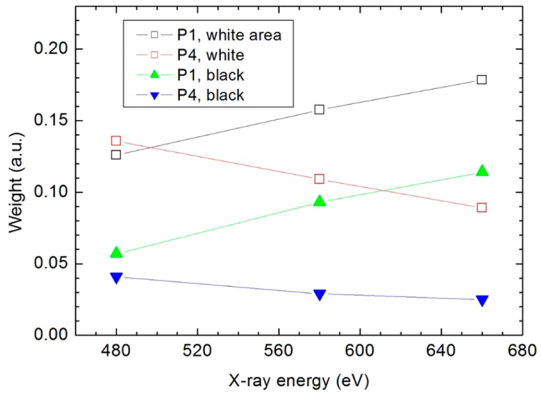

Figure 3. Spectral weight of the Nb core-level peaks P1 and P4 as a function of photon energy.

spectral weight of the P1 peak evolves oppositely to that of peak P4, with the intensity of the P1 and P4 peaks increasing and decreasing with photon energy, respectively. Not only does this confirm that the two peaks correspond to different Nb sites, it strongly suggests that the P1/P2 pair is associated with the bulk whereas the other pair is related to the surface. This observation is valid for both the white and black areas.

A contrast also exists between the As spectra recorded in the white areas (for which the bulk peaks of Nb are enhanced) and the black areas. Notably, the intensity of the As peak is reduced in the black areas. At the same time, the full width at half-maximum of this peak increases from 1.8 to 2.2 eV, with the peak enlargement occurring on the high-energy side, where the bulk components of the As core levels are reported in ARPES experiments.[5] In other words, and contrary to what we observe for the Nb peaks, the As surface states rather than the bulk states are mainly affected by the switch from the white to the black area.

Although we detect clearly the bulk states of NbAs, the interpretation of the P3 and P4 peaks in terms of the topological NbAs surface states is rather difficult to reconcile with our data. Here, we recall that the surface studied, though cleaned, is natural and it is thus subject to contamination, notably by oxygen. Nb can form different oxides, each having their own signature of Nb core levels.[13] The energies of the P3 and P4 peaks correspond well to the Nb $3d_{5/2}$ and $3d_{3/2}$ core levels in Nb_2O_5.[14] Interestingly, we observe a small bump at a binding energy of 44.6 eV that is also consistent to the 3d core levels of As in As_2O_3.[14] We believe that oxide layers of either Nb_2O_5 or As_2O_3 form in the short period before the sample insertion into the vacuum chamber. We also notice from Figure 2c,d that the weak bulk state of Nb 3d and the surface state of As 3d in As_2O_3 are more present in dark areas, indicating that the black areas are more oxidized than the white area. We conclude that for both Nb and As in NbAs, there are a bulk state at lower binding energy and a surface state at higher binding energy in the form of the oxides, which we suppose due to the binding of the free dangling bonds on the topmost surface with oxygen from air. The existence of an oxide is unexpected in our experiment, in contrast to ARPES data obtained from cleaved surfaces. By now, the literature is lacking in knowledge on the Weyl semimetal surface.

In Figure 2c, the kinetic energy of photoelectrons of Nb is about 110 eV. The corresponding mean free path of photoelectrons is about 5 Å. There is almost no bulk Nb signal present in the black area, suggesting that the black area is covered by an oxide which is thicker than 5 Å. In the white area, a nonoxidized Nb peak appears and the spectral weight of the Nb oxide becomes smaller than that in the black area. It indicates that the Nb oxide is thinner in the white area. Moreover, the kinetic energy ~280 eV of As photoelectrons in Figure 2c is comparable to the kinetic energy ~290 eV of Nb photoelectrons in Figure 2d. However, the spectral weight of the As oxide in the As 3d core level spectrum in Figure 2c is much weaker than that of the Nb oxide in the Nb 3d core level spectrum in Figure 2d, indicating that As in the black area is less oxidized, as same as in the white area. Thus, As on the surface mainly exists as NbAs bulk. Arsenide bulk intensity is much stronger in the white area than in the black area in Figure 2c,d, suggesting that the amount of NbAs is larger in the white area than in the black area.

To generate atomic percentage values (n_{Nb}/n_{As}) on the surface, each raw XPS signal must be corrected by dividing the signal intensity (I_{Nb} and I_{As}) by a relative sensitivity factor (S_{Nb} = 2.517 and S_{As} = 0.570)[15]

$$n_{Nb}/n_{As} = (I_{Nb}/S_{Nb})/(I_{As}/S_{As})$$

Our analysis suggests that n_{Nb}/n_{As} is 53.2%:46.8% for the white area, and 57.8%:42.2% for the black area. The result is unexpected because the entire area is Nb-rich as well as nonequivalent for the white and black areas. Possibly, the calculation is distorted by introduction of oxygen into the topmost surface and the underlying few layers in the form of Nb_2O_5 and As_2O_3, or due to the difference of the oxidation strength, or somehow missing As atoms from there, for example during evaporation. Though the surface may be oxidized, all previous experiments on the same batches of samples, using different techniques, suggest good quality of the NbAs bulk.[10] The difference in the elemental composition implies the possibility of coexistence of As-terminated and Nb-terminated surfaces.

Now that we have identified two types of regions at the sample surface (black and white areas), it is interesting to see what the corresponding low-energy states are, and thus we recorded complementary spectra near the Fermi level. In Figure 4, we compare the spectra associated with both regions up to 12 eV of binding energy. Although the spectra look

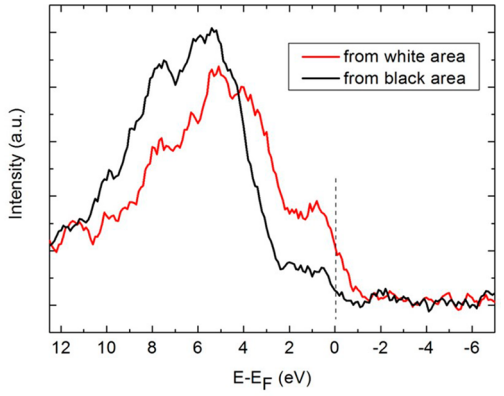

Figure 4. Comparison of the near-E_F spectra recorded with 320 eV photon energy in the white (red curve) and black (black curve) areas.

DOI: 10.1021/acs.cgd.8b00653
Cryst. Growth Des. 2018, 18, 5210−5213

roughly similar, a clear spectral weight transfer from the low to the higher binding energies is observed for the black area as compared to the white one. In particular, the spectral intensity at the Fermi level is clearly weaker for the black region. This observation supports the formation of insulating oxide at the surface in the black region, for which the spectral weight would be naturally moved away from the Fermi level.

SUMMARY

XPEEM and XPS have been utilized to investigate the spatially resolved electronic structure of Weyl semimetal NbAs surface without cleavage. XPEEM images present white and black contrasts for both the Nb 3d and As 3d images. Surface-sensitive XPS spectra show that the entire sample surface contains both surface states in the form of oxides and NbAs bulk states for both Nb 3d and As 3d. The weak bulk state of Nb 3d and the surface state of As 3d in As_2O_3 are more present in dark areas, indicating that the black areas are more oxidized than the white areas. We conclude that for both Nb and As in NbAs, there are a bulk state at lower binding energy and a surface state at higher binding energy in the form of oxides. Estimated atomic percentage values n_{Nb}/n_{As} suggest that the entire surface is Nb-rich, but the difference in the elemental composition implies the possibility of a coexistence of As-terminated and Nb-terminated surfaces.

AUTHOR INFORMATION

Corresponding Authors

*E-mail: hliu@iphy.ac.cn (H.W.L.).
*E-mail: dingh@iphy.ac.cn (H.D.).

ORCID

Hongwen Liu: 0000-0003-1974-4221

Notes

The authors declare no competing financial interest.

ACKNOWLEDGMENTS

H. W. Liu is grateful to B. Q. Lv and N. Xu for fruitful discussions. This work was supported by grants from NSFC (11674371 and 21403222) of China. This research was undertaken thanks in part to funding from the Canada First Research Excellence Fund.

REFERENCES

(1) Weyl, H. Elektron und Gravitation. I. *Eur. Phys. J. A* **1929**, *56*, 330−352.
(2) Weng, H. M.; Fang, C.; Fang, Z.; Bernevig, B. A.; Dai, X. Weyl Semimetal Phase in Noncentrosymmetric Transition-Metal Monophosphides. *Phys. Rev. X* **2015**, *5*, 011029.
(3) Lv, B. Q.; Weng, H. M.; Fu, B. B.; Wang, X. P.; Miao, H.; Ma, J.; Richard, P.; Huang, X. C.; Zhao, L. X.; Chen, G. F.; Fang, Z.; Dai, X.; Qian, T.; Ding, H. Experimental Discovery of Weyl Semimetal TaAs. *Phys. Rev. X* **2015**, *5*, 031013.
(4) Xu, S.-Y.; Alidoust, N.; Belopolski, I.; Yuan, Z.; Bian, G.; Chang, T.-R.; Zheng, H.; Strocov, V. N.; Sanchez, D. S.; Chang, G.-Q.; Zhang, C.-L.; Mou, D.-X.; Wu, Y.-W.; Huang, L.-N.; Lee, C.-C.; Huang, S.-M.; Wang, B.-K.; Bansil, A.; Jeng, H.-T.; Neupert, T.; Kaminski, A.; Lin, H.; Jia, S.; Hasan, M. Z. Discovery of a Weyl fermion state with Fermi arcs in niobium arsenide. *Nat. Phys.* **2015**, *11*, 748−754.
(5) Lv, B. Q.; Xu, N.; Weng, H. M.; Ma, J. Z.; Richard, P.; Huang, X. C.; Zhao, L. X.; Chen, G. F.; Matt, C. E.; Bisti, F.; Strocov, V. N.; Mesot, J.; Fang, Z.; Dai, X.; Qian, T.; Shi, M.; Ding, H. Observation of Weyl nodes in TaAs. *Nat. Phys.* **2015**, *11*, 724−727.
(6) Yang, L. X.; Liu, Z. K.; Sun, Y.; Peng, H.; Yang, H. F.; Zhang, T.; Zhou, B.; Zhang, Y.; Guo, Y. F.; Rahn, M.; Prabhakaran, D.; Hussain, Z.; Mo, S.-K.; Felser, C.; Yan, B.; Chen, Y. L. Weyl semimetal phase in the non-centrosymmetric compound TaAs. *Nat. Phys.* **2015**, *11*, 728−732.
(7) Xu, S.-Y.; Belopolski, I.; Alidoust, N.; Neupane, M.; Bian, G.; Zhang, C.; Sankar, R.; Chang, G.; Yuan, Z.; Lee, C.-C.; Huang, S.-M.; Zheng, H.; Ma, J.; Sanchez, D. S.; Wang, B. K.; Bansil, A.; Chou, F.; Shibayev, P. P.; Lin, H.; Jia, S.; Hasan, M. Z. Discovery of a Weyl fermion semimetal and topological Fermi arcs. *Science* **2015**, *349*, 613−617.
(8) Souma, S.; Wang, Z.; Kotaka, H.; Sato, T.; Nakayama, K.; Tanaka, Y.; Kimizuka, H.; Takahashi, T.; Yamauchi, K.; Oguchi, T.; Segawa, K.; Ando, Y. Direct observation of nonequivalent Fermi-arc states of opposite surfaces in noncentrosymmetric Weyl semimetal NbP. *Phys. Rev. B: Condens. Matter Mater. Phys.* **2016**, *93*, 161112.
(9) Xu, N.; Weng, H. M.; Lv, B. Q.; Matt, C. E.; Park, J.; Bisti, F.; Strocov, V. N.; Gawryluk, D.; Pomjakushina, E.; Conder, K.; Plumb, N. C.; Radovic, M.; Autès, G.; Yazyev, O. V.; Fang, Z.; Dai, X.; Qian, T.; Mesot, J.; Ding, H.; Shi, M. Observation of Weyl nodes and Fermi arcs in tantalum phosphide. *Nat. Commun.* **2016**, *7*, 11006.
(10) Liu, H. W.; Richard, P.; Zhao, L. X.; Chen, G.-F.; Ding, H. Comparative Raman study of Weyl semimetals TaAs, NbAs, TaP and NbP. *J. Phys.: Condens. Matter* **2016**, *28*, 295401.
(11) Griffith, D. H.; Engel, W. Historical perspective and current trends in emission microscopy, mirror electron microscopy and low-energy electron microscopy. *Ultramicroscopy* **1991**, *36*, 1−28.
(12) Locatelli, A.; Bauer, E. Recent advances in chemical and magnetic imaging of surfaces and interfaces by XPEEM. *J. Phys.: Condens. Matter* **2008**, *20*, 093002.
(13) Kuznetsov, M. V.; Razinkin, A. S.; Shalaeva, E. V. Photoelectron spectroscopy and diffraction of surface nanoscale NbO/Nb(110) structures. *J. Struct. Chem.* **2009**, *50*, 514−521.
(14) *Handbook of x-ray photoelectron spectroscopy: a reference book of standard spectra for identification and interpretation of XPS data*, Chastain, J., Ed.; Perkins-Elmer Corporation, Physical Electronics Division: Eden Prairie (MN), USA, 1995.
(15) *Practical Surface analysis, Vol. 1, Auger and X-ray Photoelectron Spectroscopy*; Briggs, D., Seah, M. P., Eds.; John Wiley and Sons: Chichester, UK, 1990.

DOI: 10.1021/acs.cgd.8b00653
Cryst. Growth Des. 2018, 18, 5210−5213